

AD-A050 598

WEAPONS RESEARCH ESTABLISHMENT SALISBURY (AUSTRALIA)  
A NEW TECHNIQUE FOR OBTAINING THE AERODYNAMICS OF MISSILES FROM--ETC(U)  
NOV 76 R L POPE  
WRE-TN-1719(WR/D)

F/G 16/4

UNCLASSIFIED

NL

1 OF 1  
AD  
A050598



AR-000-784

12

AD A 050598

WRE-TN-1719 (WR&D)



# DEPARTMENT OF DEFENCE

AUSTRALIAN DEFENCE SCIENTIFIC SERVICE

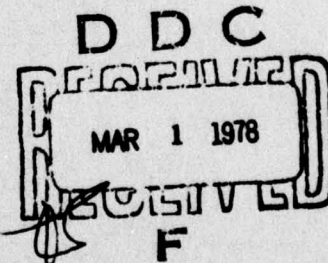
WEAPONS RESEARCH ESTABLISHMENT

SALISBURY, SOUTH AUSTRALIA

WRE-TECHNICAL NOTE-1719 (WR&D)

A NEW TECHNIQUE FOR OBTAINING THE AERODYNAMICS OF MISSILES  
FROM FLIGHT TRIALS ON A GAS GUN RANGE

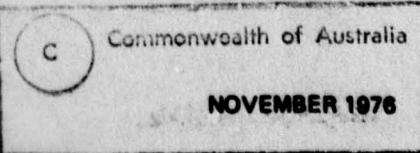
R.L. POPE



APPROVED

FOR PUBLIC RELEASE

COPY No. 86



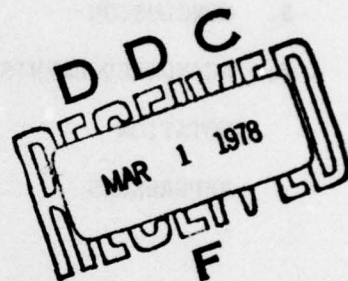
UNCLASSIFIED

DEPARTMENT OF DEFENCE  
AUSTRALIAN DEFENCE SCIENTIFIC SERVICE  
WEAPONS RESEARCH ESTABLISHMENT

WRE-TECHNICAL NOTE-1719 (WR&D)

A NEW TECHNIQUE FOR OBTAINING THE AERODYNAMICS OF MISSILES  
FROM FLIGHT TRIALS ON A GAS GUN RANGE

R.L. Pope



S U M M A R Y

This report describes a new method for obtaining the low incidence, linear aerodynamic data for a missile from very simple free flight trials on a gas gun range. The only instrumentation in the free flight model is two flashing lights, one in the nose and one in the tail. The images of these flashing lights are recorded by three ballistic cameras and the positions of the lights can then be calculated very accurately by a least squares solution of the resulting triangulation problem. The velocity of the centre of gravity and the attitude of the vehicle can be estimated from the position measurements for the nose and the tail. A parameter estimation technique using the output error criterion is applied to the attitude and velocity data to obtain aerodynamic terms. The method has been used successfully to estimate axial force, normal force, static stability and pitch damping moment for the test vehicle.

---

POSTAL ADDRESS: The Director, Weapons Research Establishment,  
Box 2151, G.P.O., Adelaide, South Australia, 5001.

---

UNCLASSIFIED



## 1. INTRODUCTION

The concept of a double flashing light vehicle grew from the single flashing light tests reported in references 1 and 2. The single flashing light technique has been used to obtain very accurate trajectories. The position data obtained with the single flashing light were so accurate that it seemed likely that useful attitude data could be obtained if longitudinally separated lights were carried. The experimental method is described in detail in Section 2. The principal ingredients are two flashing lights, which are carried in the nose and tail of the missile and three ground based ballistic cameras which are used to record the flashes along the vehicle trajectory. A set of four reference lights is used to calibrate the camera plates and the position of each flash is derived. The nose and tail positions obtained in this way are converted to centre of gravity trajectory data and attitude data, for the vehicle.

The first flight of a vehicle carrying two flashing lights was reported in reference 1. The vehicle was launched at zero incidence and the derived values of incidence were regarded as indicative of the r.m.s. noise levels and bias errors which might be present in the data from such trials. On that basis this preliminary trial showed that attitude angles could be measured with r.m.s. noise levels of less than one degree and bias errors of about half a degree. However, it was expected that the bias errors could be substantially reduced by a more accurate survey of the range.

The unexpectedly high quality of the trajectory and attitude data obtained from the first trial prompted some rethinking on the uses of the technique. As consequence the second vehicle was launched at incidence with the aim of extracting as much aerodynamic data as possible from the trial. The data analysis has been carried out using a parameter estimation technique which relies on an output error criterion. The method attempts to find values for the parameters characterising the mathematical model such that the sum of the squares of the differences between the model outputs and the measured values for attitude angles and centre of gravity velocity components is minimised. The implementation of the parameter estimation technique is outlined in Section 3.

Unfortunately, no measurements of roll orientation were made on this trial, so that only roll independent aerodynamic terms could be included in the model. Thus the model cannot represent non-linear aerodynamic terms effectively. Although minimal non-linear effects are included in the mathematical model of Section 3, they are not well determined by the data analysis. Over 90 per cent of the data points have incidence values less than six degrees. Wind tunnel data from reference 3 indicates that non-linear effects are negligible in this incidence range. The values obtained for the parameters are presented in Section 4 and comparisons are made with wind tunnel results. The accuracies obtained are surprising in view of the quality of the data; r.m.s. noise levels vary from 1% in the static aerodynamic pitching moment derivative up to 7% in the dynamic pitch damping moment derivative. The results obtained are particularly encouraging because the r.m.s. noise level in the measurements of attitude angles is between three and four times the noise level in the first experiment. Hence we expect that results from future trials will be much improved.

Section 5 presents some conclusions which are drawn from the general success of the trials technique and the data analysis. The principal conclusion concerns the next step in the development of the method. The method is restricted, by the assumption of linear aerodynamics, to treating situations where incidence amplitudes are small. In order to extend the method to treat non-linear aerodynamic terms adequately, some measure of roll orientation is required, since the non-linear contributions to the aerodynamics of finned vehicles always depend on roll angle. Plans are presently under way for testing methods of measuring roll orientation.

## 2. TRIAL

The test vehicle is depicted in figure 1 and physical data on the missile are given in Table 1. It was launched from a 385 mm bore compressed air gun at a velocity of 120 m/s and an elevation of  $20^\circ$  on a small gas gun range. The layout of the range is shown in figure 2.

The launching technique attempts to induce the missile incidence to oscillate. It is arranged in the sabot at an angle of about eight degrees, and as it emerges from the sabot air flows only over the forebody. The general effect is destabilising and the incidence increases until flow becomes established over the tail. In this way initial incidences up to  $20^\circ$  can be obtained. This provides an adequate pitching motion for later analysis. The nose and tail lights flash synchronously at 49.16 Hz, beginning at about one second after gun firing. This results in loss of some data, but the delay is necessary to allow the vehicle to clear background street lighting. The flashes are recorded by three ballistic cameras, situated as shown in figure 2. The position data is obtained from the camera records by the method outlined in reference 4.

The quality of the trajectory data is somewhat lower than expected from experience with the previous double and single flashing light trials. The estimated r.m.s. noise levels in the various parameters are given in Table 2. The main cause of the trouble may be an erratic flash rate. Some of the tail and nose flashes were inexplicably delayed and flashes were not simultaneous for about 10 points out of a total of 170, and this casts doubt on the general reliability of the flash triggering unit.

The flight history of the vehicle is given in figures 3, 4 and 5. The record available is that part of the trajectory for which a three camera solution is possible. In any case the incidence oscillation has damped to a very low amplitude by the time the vehicle moves out of view of camera one, and so the data following this are of no interest. The position and velocity histories are shown in figure 3. The velocity components are derived from the position data by simple numerical differentiation techniques outlined in reference 5. The original position and velocity data have r.m.s. noise levels which are negligible relative to the scales used in figure 3. Hence no attempt has been made to show the individual data points. The differences between the velocities obtained as model output from the parameter estimation and the measured velocities are also negligible relative to the scales of figure 3. Therefore the curves in figure 3 represent both measured data and model outputs.

Figures 4 and 5 show the angular data from the experiment. Figure 4 gives a record of the elevation and azimuth of the longitudinal axis of the vehicle and the incidence components. Figure 5 shows the behaviour of the vehicle in the incidence plane. The measured data are shown as points on these two figures and the scatter is appreciable. The corresponding outputs from the mathematical model are represented on the figures by the solid curves. These two figures provide an indication of the goodness of the fit obtained with the parameter estimation algorithm.

An outline of the method used to obtain the data presented in these figures is included here for completeness. The results are derived from simple geometrical considerations. The basic data points  $(x_T, y_T, z_T)$  and  $(x_N, y_N, z_N)$  are obtained by triangulation from the three camera records using a least squares solution. The trajectory  $(x, y, z)$  of the vehicle centre of gravity is derived from these data using the relation

$$\begin{bmatrix} x \\ y \\ z \end{bmatrix} = \begin{bmatrix} x_N \\ y_N \\ z_N \end{bmatrix} - l_{CG} \begin{bmatrix} \Delta x \\ \Delta y \\ \Delta z \end{bmatrix} \quad (1)$$

where  $l_{CG}$  is the distance of the vehicle centre of gravity aft of the flashing light at the nose, expressed as a percentage of the total distance between the lights,  $\Delta x = x_N - x_T$ , and so on. The velocity  $(\dot{x}, \dot{y}, \dot{z})$ , relative to the air, is derived from the position data using the methods outlined in Chapter V, Section 8 of reference 5 for differentiating empirical data and allowing approximately for wind. The attitude angles of yaw and pitch (or azimuth and elevation) respectively are defined by the relations

$$\begin{aligned}\tan \psi &= \Delta y / \Delta x \\ \tan \theta &= -\Delta z / [(\Delta x)^2 + (\Delta y)^2]^{1/2}\end{aligned}\quad (2)$$

and the distance between lights is given by the relation,

$$l^2 = (\Delta x)^2 + (\Delta y)^2 + (\Delta z)^2.$$

The distance  $l$  is a good measure of the reliability of the data points and of the general r.m.s. noise level in the position data. The values of  $\dot{x}$ ,  $\dot{y}$ ,  $\dot{z}$ ,  $\psi$  and  $\theta$  are used as data for the parameter estimation technique. The values of incidence in non-rolling body axes can be derived from the relations

$$\begin{bmatrix} u \\ v \\ w \end{bmatrix} = \begin{bmatrix} \cos \theta \cos \psi & \cos \theta \sin \psi & -\sin \theta \\ -\sin \psi & \cos \psi & 0 \\ \sin \theta \cos \psi & \sin \theta \sin \psi & \cos \theta \end{bmatrix} \begin{bmatrix} \dot{x} \\ \dot{y} \\ \dot{z} \end{bmatrix}\quad (3)$$

$$\tan \zeta_v = w/u$$

$$\tan \zeta_h = v/u$$

where  $u$ ,  $v$  and  $w$  are the components of vehicle velocity in rotating body axes.

### 3. PARAMETER ESTIMATION

This section provides a definition of the mathematical model used in the data analysis and outlines the method of data analysis.

#### 3.1 Mathematical model

The equations of motion for a rigid body with six degrees of freedom in non-rolling body axes are given in reference 6 in the form,

$$\begin{aligned}\dot{u} + qw - rv &= X/m - g \sin \theta, \\ \dot{v} + ru - pw &= Y/m, \\ \dot{w} + pv - qu &= Z/m + g \cos \theta, \\ \dot{\theta} &= q, \\ \dot{\psi} &= r/\cos \theta, \\ \dot{q} - Pr(1 - I_x/I) &= M/I, \\ \dot{r} + Pq(1 - I_x/I) &= N/I,\end{aligned}\quad (4)$$

where

$$\begin{bmatrix} u \\ v \\ w \end{bmatrix} = \text{velocity of vehicle in rotating body axes,}$$

$$\begin{bmatrix} p \\ q \\ r \end{bmatrix} = \text{angular velocity of vehicle in body axes,}$$

$\psi, \theta$  = angles of azimuth and elevation respectively of vehicle axis,

$$\begin{bmatrix} X \\ Y \\ Z \end{bmatrix} = \text{aerodynamic forces,}$$

$$\begin{bmatrix} L \\ M \\ N \end{bmatrix} = \text{aerodynamic moments,}$$

$P = -r \tan \theta$  = residual roll rate of axes,

$m$  = vehicle mass, and

$I_x, I$  = moments of inertia of vehicle in roll and pitch, respectively.

The non-rolling body axes have the OX axis forward along the longitudinal body axis, the OY axis in a horizontal plane to the right, and the OZ axis completes the right handed set. In order to maintain the OY axis in a horizontal plane a small residual roll rate must be maintained for the axes system, this axes roll rate is called P, in contrast to the body roll rate, p, which does not appear in the equations because of the assumption that the roll equation is uncoupled from the other equations. Since there is no roll information available, the body roll rate and roll position equations are omitted and it is assumed that the roll dependence of the aerodynamic forces and moments is negligible. Ninety per cent of the data is taken for incidence values less than six degrees in the particular example treated here so that this assumption is unlikely to introduce any errors larger than the r.m.s. values. Similarly, although the first non-linear terms in incidence variation of restoring moment and normal force are included, we cannot expect to determine them reliably because there is insufficient high incidence data.

The expressions for the aerodynamic forces and moments are,

$$X = QSC_X$$

$$Y = QS(C_{Z_\xi} + C_{Z_{\xi^3}} \tan^2 \xi) v/u$$

$$Z = QS(C_{Z_\xi} + C_{Z_{\xi^3}} \tan^2 \xi) w/u$$

$$\begin{aligned} M &= QSd[(C_{m_\xi} + C_{m_{\xi^3}} \tan^2 \xi) w/u + C_{m_q} (qd/2V)] \\ N &= QSd[(C_{m_\xi} + C_{m_{\xi^3}} \tan^2 \xi) v/u + C_{m_q} (rd/2V)] \end{aligned} \quad (5)$$

where

$$\tan^2 \xi = (v^2 + w^2)/u^2$$

$$C_{m_\xi} \tan \xi + C_{m_{\xi^3}} \tan^3 \xi = \text{aerodynamic pitching moment coefficient,}$$

$$C_{Z_\xi} \tan \xi + C_{Z_{\xi^3}} \tan^3 \xi = \text{aerodynamic normal force coefficient,}$$

$$C_X = \text{aerodynamic axial force coefficient,}$$

$$C_{m_q} = \text{aerodynamic pitch damping derivative,}$$

$$Q = \text{dynamic pressure,}$$

$$S = \text{force and moment reference area and}$$

$$d = \text{body diameter.}$$

It should be noted that the Mach number is less than 0.4 so that the flow is incompressible and there is no variation of any of the coefficients  $C_X$ , etc. with Mach number. The terms  $C_{m_\xi}$ ,  $C_{m_{\xi^3}}$ ,  $C_{Z_\xi}$ ,  $C_{Z_{\xi^3}}$  are derived from the

Taylor series expansions for the static aerodynamic pitching moment and normal force. The vehicle flies at low subsonic Mach numbers, throughout the flight, and we have assumed that there is no roll dependence of aerodynamic terms. Therefore the pitching moment and normal force coefficients are functions of  $\tan \xi$  only. As the majority of the data points show only low values of incidence ( $\tan \xi \leq 0.1$ ) we can use Taylor series expansions for normal force and pitching moment. Allowing for the fact that both are odd functions of  $\xi$ , we obtain the expansions used above,

$$C_m = C_{m_\xi} \tan \xi + C_{m_{\xi^3}} \tan^3 \xi + \dots$$

$$C_Z = C_{Z_\xi} \tan \xi + C_{Z_{\xi^3}} \tan^3 \xi + \dots$$

for pitching moment and normal force coefficients, respectively

Then  $\psi, \theta$  are obtained directly, as model outputs and the velocities  $\dot{x}, \dot{y}, \dot{z}$  are obtained from the simple axis transformation

$$\begin{bmatrix} \dot{x} \\ \dot{y} \\ \dot{z} \end{bmatrix} = \begin{bmatrix} \cos \theta \cos \psi & -\sin \psi & \sin \theta \cos \psi \\ \cos \theta \sin \psi & \cos \psi & \sin \theta \sin \psi \\ -\sin \theta & 0 & \cos \theta \end{bmatrix} \begin{bmatrix} u \\ v \\ w \end{bmatrix} \quad (6)$$

which is the inverse of equation (3). These five quantities can then be compared with values for the same variables which have been obtained from the trajectory measurements. The initial values  $\dot{x}_0, \dot{y}_0, \dot{z}_0, \psi_0, \theta_0, q_0, r_0$  which are required to start the numerical integration of equations (4) are parameters which must be determined by the parameter estimation process, in addition to values for the aerodynamic parameters  $C_X, C_{Z_f}, C_{Z_{f3}}, C_{m_f}, C_{m_{f3}}$  and  $C_{m_q}$ . The parameters are referred to as  $p_1, p_2, \dots, p_{13}$  in the rest of this report and are taken in the order given above, where  $p_1 = \dot{x}_0$ , and so on up to  $p_{13} = C_{m_q}$ . Table 3 can be used as a guide to the parameters represented by each  $p_i$ . The above equations and parameters thus define the whole mathematical model used in the parameter estimation process.

### 3.2 Normal equations

The technique for adjusting initial guesses for parameter values is essentially a modified Newton-Raphson technique as discussed in reference 7, but it is outlined here for completeness. If there are measured values

$$m_{ij} = m_j(p_1, p_2, \dots, p_N, t_i) \text{ for } i = 1, 2, \dots, I, j = 1, \dots, J$$

of  $J$  flight variables at  $I$  times  $t_i$ , where  $IJ > N$ , the parameters  $p_1, p_2, \dots, p_N$  can be obtained by a recursive solution of a set of normal equations which are derived below.

Assuming that we have a current set of estimates  $p_n^{(s)}$ ,  $n = 1, 2, \dots, N$  for the parameter values, then by using the mathematical model we can estimate a set of measurements by numerical integration of the model equations, and they are,

$$m_{ij}^{(s)} = m_j(p_1^{(s)}, p_2^{(s)}, \dots, p_N^{(s)}, t_i).$$

This set can be used to form a vector of residuals  $R^{(s)}$  where each element

$$r_k^{(s)} = m_{ij} - m_{ij}^{(s)} \quad k = 1, 2, \dots, IJ = K \quad (7)$$

where

$$k = (i - 1) J + j$$

Then the output error method of parameter estimation requires the the quantity

$$U^{(s)} = R^{(s)T} W R^{(s)} \quad (8)$$

is minimised, where  $W$  is a weighting matrix. The matrix  $W$  is a  $K \times K$  diagonal matrix, and the values on the diagonal are proportional to the accuracy of each measurement.

Suppose that new parameter values can be represented by the relations

$$p_n^{(s+1)} = p_n^{(s)} + \delta p_n, \quad (9)$$

so that the new set of estimates for the measurements can be written in the form

$$m_k^{(s+1)} = m_k^{(s)} + \sum_{n=1}^N \frac{\partial m_k^{(s)}}{\partial p_n} \delta p_n + O[(\delta p_n)^2], \quad (10)$$

using the Taylor series expansion, where  $k$  is defined in equation (7). Now the sum of squares of residuals is given by

$$U^{(s+1)} = R^{(s+1)T} W R^{(s+1)} \quad (11)$$

where  $r_k^{(s+1)} = m_k - m_k^{(s+1)}$ , and the aim of the method is to minimise  $U^{(s+1)}$ .

The minimum occurs when  $\partial U^{(s+1)} / \partial (\delta p_n) = 0$  for all  $n$ . The Taylor series expansion from equation (10) can be written in the form

$$M^{(s+1)} = M^{(s)} + D^{(s)} E \quad (12)$$

where  $D^{(s)}$  is a matrix of partial derivatives, such that  $d_{kn} = \partial m_k^{(s)} / \partial p_n$ ,  $M^{(s)}$  is a vector of model outputs  $m_k^{(s)}$  and  $E$  is a matrix of unknown parameter adjustments  $\delta p_n$ . Since  $R^{(s)} = M - M^{(s)}$ , where  $M$  is the vector of measured values the above equation for the Taylor series expansion can be rewritten in the form

$$R^{(s+1)} = R^{(s)} - D^{(s)} E. \quad (13)$$

Then using this to substitute in the equation (12) for  $U^{(s+1)}$ , we find that

$$U^{(s+1)} = (R^{(s)T} - E^T D^{(s)T}) W (R^{(s)} - D^{(s)} E)$$

and hence it follows from the conditions for a minimum,

$$\partial U^{(s+1)} / \partial (\delta p_n) = 0 \text{ for all } n,$$

that

$$-2 D^{(s)T} W R^{(s)} + 2 D^{(s)T} W D^{(s)} E = 0. \quad (14)$$

Therefore, if we represent the positive definite matrix  $D^{(s)T} W D^{(s)}$ , by  $\Psi$ , the normal equations have the form

$$\Psi E = D^{(s)T} W R^{(s)}, \quad (15)$$

which gives the solution

$$E = \Psi^{-1} D^{(s)T} W R^{(s)} \quad (16)$$

thus yielding values for the parameter increments  $\delta p_n$ .

Some statistics are available on the accuracy and reliability of the updated estimates of the parameter values. The following results are quoted from reference 7. An estimate of the r.m.s. value  $\sigma$ , of the residuals, or the value of  $U^{(s+1)}$ , the sum of squares of the residuals using the updated parameter estimates is given by

$$\sigma^2 = \sigma_0^2 - E^T D^{(s)T} W R^{(s)} \quad (17)$$

where  $\sigma_0^2$  is r.m.s. of the residuals of the observations using uncorrected parameters. The covariance matrix of the parameters is given by

$$\text{cov}(E) = \sigma^2 \Psi^{-1},$$

and this is particularly useful in determining when parameter values are correlated, because in such cases estimated values of the correlated parameters are unreliable. Finally the accuracy of each parameter estimate can be determined from the standard deviation or r.m.s. error level  $\sigma(p_n)$

which is given by

$$\sigma^2(p_n) = \sigma^2 \Psi_{nn}^{-1} \quad (18)$$

where  $\Psi_{nn}^{-1}$  is the  $n^{\text{th}}$  diagonal element of  $\Psi^{-1}$ .

### 3.3 Partial derivatives

An important requirement of the parameter estimation technique outlined above is to estimate the partial derivatives of the estimates of the observed values, with respect to the parameters. There are alternative methods of approach, but the most effective presently available seems to be to use partial differentiation of equations (4) and (5) which define the mathematical model in Section 3.1. This approach yields the following simultaneous differential equations, for  $j = 1, 2, \dots, 13$ ,

$$\begin{aligned} \frac{d}{dt} \left( \frac{\partial u}{\partial p_j} \right) &= -q \frac{\partial w}{\partial p_j} - w \frac{\partial q}{\partial p_j} + r \frac{\partial v}{\partial p_j} + v \frac{\partial r}{\partial p_j} + \frac{QS}{m} \delta_{8j} - g \cos \theta \frac{\partial \theta}{\partial p_j} \\ \frac{d}{dt} \left( \frac{\partial v}{\partial p_j} \right) &= -r \frac{\partial u}{\partial p_j} - u \frac{\partial r}{\partial p_j} + p \frac{\partial w}{\partial p_j} + w \frac{\partial p}{\partial p_j} + \frac{QS}{mu} [ (p_9 + p_{10} \tan^2 \zeta) \frac{\partial v}{\partial p_j} \\ &\quad + (\delta_{9j} + \delta_{10j} \tan^2 \zeta) v + 2p_{10} \frac{v}{u^2} (v \frac{\partial v}{\partial p_j} + w \frac{\partial w}{\partial p_j}) ] \end{aligned} \quad (19)$$

$$\begin{aligned} \frac{d}{dt} \left( \frac{\partial w}{\partial p_j} \right) &= -p \frac{\partial v}{\partial p_j} - v \frac{\partial p}{\partial p_j} + q \frac{\partial u}{\partial p_j} + u \frac{\partial q}{\partial p_j} + \frac{QS}{mu} [ (p_9 + p_{10} \tan^2 \zeta) \frac{\partial w}{\partial p_j} \\ &\quad + (\delta_{9j} + \delta_{10j} \tan^2 \zeta) w + 2p_{10} \frac{w}{u^2} (v \frac{\partial v}{\partial p_j} + w \frac{\partial w}{\partial p_j}) ] - g \sin \theta \frac{\partial \theta}{\partial p_j} \end{aligned}$$

$$\frac{d}{dt} \left( \frac{\partial \theta}{\partial p_j} \right) = \frac{\partial q}{\partial p_j}$$

$$\frac{d}{dt} \left( \frac{\partial \psi}{\partial p_j} \right) = \sec \theta \frac{\partial r}{\partial p_j} + r \sec \theta \tan \theta \frac{\partial \theta}{\partial p_j}$$

$$\begin{aligned} \frac{d}{dt} \left( \frac{\partial q}{\partial p_j} \right) &= (1 - I_x/I) (p \frac{\partial r}{\partial p_j} + r \frac{\partial p}{\partial p_j}) + \frac{QSd}{Iu} \{ (p_{11} + p_{12} \tan^2 \zeta) \frac{\partial w}{\partial p_j} \\ &\quad + (\delta_{11j} + \delta_{12j} \tan^2 \zeta) w + 2p_{12} \frac{w}{u^2} (v \frac{\partial v}{\partial p_j} + w \frac{\partial w}{\partial p_j}) \\ &\quad + \frac{1}{2} p_{13} d \frac{\partial q}{\partial p_j} + \frac{1}{2} qd \delta_{13j} \} \end{aligned}$$

$$\begin{aligned} \frac{d}{dt} \left( \frac{\partial r}{\partial p_j} \right) &= -(1 - I_x/I) (p \frac{\partial q}{\partial p_j} + q \frac{\partial p}{\partial p_j}) + \frac{QSd}{Iu} \{ -(p_{11} + p_{12} \tan^2 \zeta) \frac{\partial v}{\partial p_j} \\ &\quad - (\delta_{11j} + \delta_{12j} \tan^2 \zeta) v - 2p_{12} \frac{v}{u^2} (v \frac{\partial v}{\partial p_j} + w \frac{\partial w}{\partial p_j}) \\ &\quad + \frac{1}{2} p_{13} d \frac{\partial r}{\partial p_j} + \frac{1}{2} dr \delta_{13j} \} \end{aligned}$$

where  $\partial P / \partial p_j = -\tan \theta \partial r / \partial p_j - r \sec^2 \theta \partial \theta / \partial p_j$ . The partial derivatives for  $\psi$  and  $\theta$  come directly from this set of differential equations. The partial derivatives for  $\dot{x}$ ,  $\dot{y}$  and  $\dot{z}$  must be derived from the axes transformation, given in Section 3.1,

$$\begin{bmatrix} \dot{x} \\ \dot{y} \\ \dot{z} \end{bmatrix} = \begin{bmatrix} \cos \theta \cos \psi & -\sin \psi & \sin \theta \cos \psi \\ \cos \theta \sin \psi & \cos \psi & \sin \theta \sin \psi \\ -\sin \theta & 0 & \cos \theta \end{bmatrix} \begin{bmatrix} u \\ v \\ w \end{bmatrix}$$

Partial differentiation of this relation yields

$$\begin{aligned} \frac{\partial \dot{x}}{\partial p_j} &= \frac{\partial u}{\partial p_j} \cos \theta \cos \psi - \frac{\partial v}{\partial p_j} \sin \psi + \frac{\partial w}{\partial p_j} \sin \theta \cos \psi - \dot{y} \frac{\partial \psi}{\partial p_j} \\ &\quad + \dot{z} \cos \psi \frac{\partial \theta}{\partial p_j} \\ \frac{\partial \dot{y}}{\partial p_j} &= \frac{\partial u}{\partial p_j} \cos \theta \sin \psi + \frac{\partial v}{\partial p_j} \cos \psi + \frac{\partial w}{\partial p_j} \sin \theta \sin \psi + \dot{x} \frac{\partial \psi}{\partial p_j} \\ &\quad + \dot{z} \sin \psi \frac{\partial \theta}{\partial p_j} \end{aligned} \quad (20)$$

$$\frac{\partial \dot{z}}{\partial p_j} = -\frac{\partial u}{\partial p_j} \sin \theta + \frac{\partial w}{\partial p_j} \cos \theta - (u \cos \theta + w \sin \theta) \frac{\partial \theta}{\partial p_j}$$

The set of simultaneous, ordinary differential equations in partial derivatives given in equation (19) with the equations of motion quoted in equation (4) comprise the complete mathematical model and form the complete set of 98 first order simultaneous differential equations (for 13 parameters) which must be solved on each iteration of the parameter estimation method so that 98 initial values are required to start the solution. The first six parameters represent the initial values  $\dot{x}_0$ ,  $\dot{y}_0$ ,  $\dot{z}_0$ ,  $\psi_0$ ,  $\theta_0$ ,  $q_0$ ,  $r_0$  in that order. The inverse transform to that stated above is required to find  $(u_0, v_0, w_0)$  and the inverse is obtained simply by transposing the matrix so that

$$\begin{bmatrix} u_0 \\ v_0 \\ w_0 \end{bmatrix} = \begin{bmatrix} \cos \theta_0 \cos \psi_0 & \cos \theta_0 \sin \psi_0 & -\sin \theta_0 \\ -\sin \psi_0 & \cos \psi_0 & 0 \\ \sin \theta_0 \cos \psi_0 & \sin \theta_0 \sin \psi_0 & \cos \theta_0 \end{bmatrix} \begin{bmatrix} \dot{x}_0 \\ \dot{y}_0 \\ \dot{z}_0 \end{bmatrix} \quad (21)$$

The initial values for some of the partial derivatives are rather more complex. First the simple ones are

$$\left. \frac{\partial \psi}{\partial p_j} \right|_{t=0} = \delta_{4j}, \left. \frac{\partial \theta}{\partial p_j} \right|_{t=0} = \delta_{5j}, \left. \frac{\partial q}{\partial p_j} \right|_{t=0} = \delta_{6j}, \left. \frac{\partial r}{\partial p_j} \right|_{t=0} = \delta_{7j}$$

where  $\delta_{ij}$  is the Kronecker delta symbol; 1 when  $i = j$  and 0 otherwise.

The other initial conditions must be obtained through the axes transformation and are as follows,

$$\begin{aligned} \left. \frac{\partial u}{\partial p_1} \right|_{t=0} &= \cos \theta_0 \cos \psi_0, & \left. \frac{\partial u}{\partial p_2} \right|_{t=0} &= \cos \theta_0 \sin \psi_0, & \left. \frac{\partial u}{\partial p_3} \right|_{t=0} &= -\sin \theta_0, \\ \left. \frac{\partial u}{\partial p_4} \right|_{t=0} &= v_0 \cos \theta_0, & \left. \frac{\partial u}{\partial p_5} \right|_{t=0} &= -w_0, & \left. \frac{\partial u}{\partial p_j} \right|_{t=0} &= 0 \text{ for } j \geq 6, \\ \left. \frac{\partial v}{\partial p_1} \right|_{t=0} &= -\sin \psi_0, & \left. \frac{\partial v}{\partial p_2} \right|_{t=0} &= \cos \psi_0, & \left. \frac{\partial v}{\partial p_3} \right|_{t=0} &= 0, \\ \left. \frac{\partial v}{\partial p_4} \right|_{t=0} &= -\dot{x}_0 \cos \psi_0 + \dot{y}_0 \sin \psi_0, & \left. \frac{\partial v}{\partial p_5} \right|_{t=0} &= 0, & \left. \frac{\partial v}{\partial p_j} \right|_{t=0} &= 0 \text{ for } j \geq 6, \\ \left. \frac{\partial w}{\partial p_1} \right|_{t=0} &= \sin \theta_0 \cos \psi_0, & \left. \frac{\partial w}{\partial p_2} \right|_{t=0} &= \sin \theta_0 \sin \psi_0, & \left. \frac{\partial w}{\partial p_3} \right|_{t=0} &= \cos \theta_0, \\ \left. \frac{\partial w}{\partial p_4} \right|_{t=0} &= v_0 \sin \theta_0, & \left. \frac{\partial w}{\partial p_5} \right|_{t=0} &= u_0 \text{ and} & \left. \frac{\partial w}{\partial p_j} \right|_{t=0} &= 0 \text{ for } j \geq 6. \end{aligned}$$

### 3.4 Algorithm implementation

The algorithm proceeds as follows. We wish to set up and solve the normal equations (15), which are a set of  $N$  linear simultaneous equations for the unknown perturbations in the parameter values  $p_j$ ,  $j = 1, 2, \dots, N$ . The normal equations (15) can be rewritten in the form

$$A \underline{x} = \underline{b}$$

where  $\underline{x}$  is the column vector of unknown parameter perturbations,  $A$  is the matrix of partial derivatives and  $\underline{b}$  is a column vector of residuals. The matrix,  $A$ , has members

$$a_{nm} = \sum_{i=1}^I \sum_{j=1}^5 \sum_{k=1}^I \sum_{l=1}^5 \frac{\partial m_{ij}}{\partial p_n}^{(s)} \frac{\partial m_{kl}}{\partial p_m}^{(s)} w_j w_l$$

and the vector,  $\underline{b}$ , has members

$$b_n = \sum_{i=1}^I \sum_{j=1}^5 \frac{\partial m_{ij}}{\partial p_n}^{(s)} (m_{ij} - m_{ij}^{(s)}) w_j$$

where  $n, m = 1, 2 \dots N$ , where  $N$  is the number of parameters being sought. The measurements  $m_{ij}$  represent the measured values of  $\dot{x}, \dot{y}, \dot{z}$ , and  $\theta$  at time  $t_i$ , so that  $m_{i1} = \dot{x}(t_i)$ , for  $i = 1, 2, \dots I$  and so on up to  $m_{i5} = \theta(t_i)$ , for  $i = 1, 2, \dots I$ . The weights  $w_j$  for  $j = 1, 2, \dots 5$  are proportional to the accuracies in the measured variables  $\dot{x}, \dot{y}, \dot{z}, \psi$  and  $\theta$ . The values for the partial derivatives  $\partial m_{ij}^{(s)} / \partial p_n$  can be obtained from the numerical solutions of the mathematical model equations (19), for the partial derivatives and by using the transformation equation (20). The model outputs  $m_{ij}^{(s)}$  used to evaluate the vector of residuals,  $b$ , can be obtained from the numerical solutions of the mathematical model equations (4) and the axes transformations equation (6). Then the normal equations can be solved for the perturbations to the parameter values and the next iteration of the algorithm begun.

The normal equations discussed above simply tell us how to improve our estimates of the parameter values. Two major problems remain. First, how to choose first values for the parameters, and second, how to control the algorithm so as to encourage convergence rather than divergence. The problem of choosing initial values is not very difficult. The initial values of velocity, angular displacements and angular velocities can be estimated reasonably well from the data. Apart from this, only  $C_{m\dot{\gamma}}$  is really required;

the remaining values can be started at zero. The pitching moment derivative  $C_{m\dot{\gamma}}$  can be easily estimated from the relation

$$\omega^2 = Q S d C_{m\dot{\gamma}} / I$$

where  $\omega$  is the frequency in radians per second of the pitching oscillations shown in figures 4 and 5. Methods for obtaining convergence are difficult to express in simple general rules, since they will vary with the problem being treated. However a basic technique is to avoid trying to find values for all parameters at once. A general approach is to arrange the parameters in order of importance of their effect on the motion or model outputs. Then only the first two or three should be allowed to vary and convergence obtained for that situation. When convergence has been reached two or three of the other parameters should also be allowed to vary until convergence is achieved once again. The process should be allowed to proceed in this way until all parameters have been determined and the solution optimised.

#### 4. RESULTS

The parameter values obtained from the parameter estimation analysis of the trials results are given in Table 3, together with the estimated root mean square errors in each. These values were obtained using 150 points out of the total of 157 which were finally available, beginning at the seventh flash. A weight of 0.1 was used in matching against the velocity components relative to a weight of unity for the angular data. This can be related to the r.m.s. noise levels given in Table 2 which show in broad terms that noise levels are an order greater, numerically, in velocity components, than in attitude angles, although much less in percentage terms.

The accuracy of the fit obtained in terms of measured data and model outputs is apparent from figures 3, 4 and 5. Figure 3 shows velocities and on the scales used the differences between measured values and model outputs are

negligible. Figures 4 and 5 show angular data both attitude angles and incidence angles. Here the noise in the data is appreciable and the scatter of the data points compared with the amplitude of the oscillation provides a good idea of how well the parameter estimation method has matched the data. The figures also show that substantial improvements can be expected in the accuracy of derived aerodynamic coefficients, if the noise levels in the angular data are nearer the expected value of one degree, rather than three or four degrees.

Table 3 shows that initial values of state variables are well determined. However the quantities of main interest are the aerodynamic coefficients. The drag coefficient is well determined with an r.m.s. error of only 2.2%, as is also the pitching moment derivative at zero incidence,  $C_{m\dot{\gamma}}$ , with an r.m.s.

error of 0.9%. The normal force derivative near zero incidence and the pitch damping derivative are less well determined, with r.m.s. errors around 7%. The derivation of normal force depends mainly on velocity measurements and the insensitivity of the changes in velocity to this parameter is reflected in the low accuracy of the normal force derivative. Since 90% of the data was taken at incidence amplitudes less than six degrees the information on non-linear normal force and pitching moment terms,  $C_{Z\dot{\gamma}^3}$  and  $C_{m\dot{\gamma}^3}$ , was minimal. In fact,

attempts to determine the non-linear terms produced values with r.m.s. errors of between 20 and 50% while simultaneously doubling the uncertainty in the linear terms. Therefore the attempts were abandoned.

Some effort was made to verify the results by comparison with wind tunnel measurements given in reference 3. The principal wind tunnel results are plotted in figures 6 and 7 which show pitching moment coefficient and axial and normal force coefficients respectively. Unfortunately there were some differences between the flight model, shown in figure 1 and the model used in wind tunnel measurements. The first and most obvious is the cylindrical cap which houses the rear flashing light. However, it is estimated that this will not produce appreciable effects on the aerodynamic coefficients. The second difference which is more important is that the fins on the flight model are only 0.018 calibres thick, whereas the fins on the wind tunnel model are 0.031 calibres thick. Consequently the chamfer on the leading edge of the flight model reaches only about halfway to the junction of the boattail and cylindrical tail section of the body, while the chamfer on the wind tunnel model reaches the junction exactly. This raises the possibility of separation from the leading edge of the fins due to the unfavourable pressure gradients produced, and a consequent loss in efficiency of the tail of the free flight model. Two other differences between wind tunnel tests and the flight test, which would probably affect drag only are the Reynolds number, and the roughness band which was used on the wind tunnel model to induce a turbulent boundary layer. The Reynolds number based on body diameter was  $2.94 \times 10^5$  for the wind tunnel tests and varied from  $1.437 \times 10^6$  down to  $1.317 \times 10^6$  in the flight tests.

Let us look first at the axial force coefficient  $C_x$ . The value obtained from wind tunnel measurements is  $(C_x)_{WT} = 0.123$  and the value obtained from this free flight experiment is  $(C_x)_{FF} = 0.100$ , a value which is further supported by the measurement of 0.097 obtained from the previous trial reported in reference 1. As far as axial force is concerned the main difference between the wind tunnel measurements and the free flight trials is the Reynolds number. The skin friction contribution to the drag on a flat plate varies with Reynolds number, according to the relation

$$C_f \propto (\log_{10} Re)^{-2.45}$$

Since the skin friction contributes about 85% of the axial force on the model, the corrected value of the free flight measurement for a Reynolds number equivalent to the wind tunnel value is  $(C_x)_{EQ} = 0.126$ . Allowances for the effects of thinner fins and absence of a roughness band on the free flight model would increase this estimate slightly. However, the differences between the value corrected for Reynolds number and the value measured in the wind tunnel would remain within the experimental error limits.

The normal force derivative measured in free flight was  $(C_{Z_f})_{FF} = -3.5$ , while wind tunnel measurements gave  $(C_{Z_f})_{WT} = -4.2$  a difference of 0.7.

However, the r.m.s. error in the flight measurement is 0.24, so that the difference is less than three standard deviations, assuming that the error distribution is normal. While such a discrepancy is by no means probable it is not, statistically, highly significant. On the other hand flight measurements gave  $(C_{m_f})_{FF} = -3.8$ . The discrepancy here is 0.5 compared with an r.m.s. error

of 0.03, so that the difference is clearly significant. However, since the moment arm for the tail lift is about twice that for the nose, relatively small variations in tail efficiency result in relatively large changes in static stability, and so it seems likely that this discrepancy can be accounted for by some small additional separation on the fins of the free flight model due to the slight differences in the leading edge chamfer. In fact only seven per cent loss of efficiency of the tail will lead to the values of  $C_{m_f}$  obtained from the

free flight experiment. This results in a loss of only 3.5% of total lift. Examination of figure 1 shows that lift could easily be lost from seven per cent of the fin area due to separations arising from the fact that the leading edge chamfer falls short of the end of the boat tail. Such a result is of course also consistent with the value obtained for  $C_{Z_f}$ , although the r.m.s. errors in

$C_{Z_f}$  are so large that nothing definite can be said about values obtained for normal force.

Thus, as far as can be ascertained, the free flight experimental results are consistent with wind tunnel measurements. Although there are some discrepancies, they can be accounted for by differences between the two models. In addition, the axial force coefficient measurement compares well with the value of 0.095 derived from a previous flight(ref.1) during which the model achieved no significant incidence.

## 5. CONCLUSION

A simple, cheap and convenient technique for flight testing of missile shapes has been presented. The advantages of the technique arise from the large amount of information which can be derived from relatively few measurements. The only on board facilities required are two flashing lights and a small flash initiator unit. The vehicle is launched from a compressed air gun, and the light flashes are recorded by three ballistic cameras. Values for all the important aerodynamic derivatives can be derived from the experimental data, using a parameter estimation technique. The steps in gathering and analysing the data are all simple and straightforward although some, such as reading the camera plates are somewhat onerous and exacting.

Comparing the free flight results with wind tunnel measurements shows some discrepancies. However, the difference between wind tunnel values and free flight values for the aerodynamic derivatives can be explained by differences between the two models used, and by Reynolds number effects.

At this stage of development of the flashing light technique it is possible to measure all the significant aerodynamic derivative values near zero incidence, that is, all the significant linear aerodynamic terms. The next step is to take some account of the non-linear aerodynamic effects which become significant at higher values of incidence. Non-linear aerodynamic effects are always dependent on the orientation of the vehicle relative to the incidence plane. Hence, in order to extend the usefulness of the technique, a means of measuring the roll orientation of the vehicle needs to be developed. This may require the inclusion of telemetry in the system, although this should be avoided if at all possible because both the free flight vehicle and the data collection and analysis will then become much more complicated and expensive. However, if the method is to be generally useful some means of measuring roll orientation of the vehicle will have to be found.

## 6. ACKNOWLEDGEMENTS

I would like to thank Mr R.E. Dudley of Field Experiments Group for his contribution to the work reported here. He has organised and conducted all the flashing light trials and the high accuracy of the results is in large part due to his efforts. I would also like to thank the staff of Planning and Data Analysis Group, who accurately read and interpreted the ballistic camera plates.

## NOTATION

$C_f$	skin friction coefficient
$C_X$	axial force coefficient
$C_{Z_\xi}$	linear normal force coefficient
$C_{Z_\xi^3}$	non linear normal force coefficient
$C_{m_\xi}$	linear restoring moment coefficient
$C_{m_\xi^3}$	non linear restoring moment coefficient
$C_{m_q}$	pitch damping coefficient
$d$	body diameter
$g$	gravitational acceleration
$I_x$	moment of inertia in roll
$I$	moment of inertia in pitch
$\begin{bmatrix} L \\ M \\ N \end{bmatrix}$	total aerodynamic moments
$l$	vehicle length - distance between lights
$l_{CG}$	distance of centre of gravity aft of nose light, as a fraction of total distance between lights
$m$	vehicle mass
$m_k$	measured values
$P$	residual roll rate of body axes
$\begin{bmatrix} p \\ q \\ r \end{bmatrix}$	angular velocity vector of body
$Re$	Reynolds number
$p_i$	parameters to be estimated
$\delta p$	changes to parameters
$Q$	dynamic pressure
$r_k$	residual errors in estimated measurements
$S$	reference area for aerodynamic forces and moments

$t$	time
$\begin{bmatrix} u \\ v \\ w \end{bmatrix}$	vehicle velocity vector in rotating body axes
$\begin{bmatrix} X \\ Y \\ Z \end{bmatrix}$	total aerodynamic forces
$\begin{bmatrix} x \\ y \\ z \end{bmatrix}$	vehicle position in range axes
$\begin{bmatrix} \Delta x \\ \Delta y \\ \Delta z \end{bmatrix}$	differences between nose and tail positions
$\xi$	total vehicle incidence
$\xi_h$	horizontal incidence component
$\xi_v$	vertical incidence component
$\theta$	elevation angle for vehicle attitude
$\sigma$	r.m.s. error levels
$\Psi$	matrix in normal equations
$\psi$	azimuth angle for vehicle attitude
$\omega$	frequency of pitching oscillation (rad/s)
superscripts	
$\cdot$	differentiation with respect to time
$(s)$	estimate using current parameter values
subscripts	
$o$	initial values
$N$	values pertaining to nose light trajectory
$T$	values pertaining to tail light trajectory

## REFERENCES

No.	Author	Title
1	Jepps, G. and Pope, R.L.	"Sub-munition scatter research 1973-1975". WRE-Report-1705 (WR&D), October 1976 (Restricted)
2	Pope, R.L.	"Use of precision trajectories to determine missile flight behaviour". WRE-TN-1704 (WR&D), March 1977
3	Robinson, M.L.	Unpublished wind tunnel data
4	Roughan, J.L.	Computation of vehicle position from several cameras". WRE-TN-558 (T), December 1971
5	Lanczos, C.	"Applied Analysis". Pitman & Sons (London) 1957
6	Goodale, P.L.	"An IBM 7090 six degrees of freedom rigid body trajectory programme". WRE TN HSA 118, June 1966
7	Waterfall, A.P.	"A technique for the automatic digital analysis of flight dynamic response data". RAE Technical Report 70228, November 1970

TABLE 1. MISSILE PHYSICAL DATA

Mass	17.9 kg
Roll inertia	0.046 kg m <sup>2</sup>
Pitch inertia	1.34 kg m <sup>2</sup>
Diameter (calibre)	0.175 m
Reference Area	0.02405 m <sup>2</sup>
Centre of gravity	2.39 calibres from nose

TABLE 2. MEAN R.M.S. NOISE LEVELS ON TRAJECTORY DATA

Variable	Nose	Tail	CG
x (m)	0.013	0.038	-
y (m)	0.010	0.048	-
z (m)	0.018	0.065	-
$\dot{x}$ (m/s)	0.47	1.23	0.47
$\dot{y}$ (m/s)	0.49	1.11	0.45
$\dot{z}$ (m/s)	0.32	0.86	0.40
$\psi$ (rad)	-	-	0.045
$\theta$ (rad)	-	-	0.071

Note: The length of the vehicle calculated from nose and tail trajectories has a mean, 1.077 m, and a standard deviation, 0.0280 m. If we assume that nose and tail trajectories contribute equally to the standard deviation then the range coordinates, which are the most significant in determining vehicle length, must have an r.m.s. noise level which averages 0.0198 m. Although a little large, this is reasonably consistent with the above table.

TABLE 3. DERIVED PARAMETER VALUES

Parameter	Variable	Value	r.m.s. error
1	$\dot{x}_0$ (m/s)	120.15	0.058
2	$\dot{y}_0$ (m/s)	-1.64	0.040
3	$\dot{z}_0$ (m/s)	-36.29	0.059
4	$\psi_0$ (rad)	0.034	0.0068
5	$\theta_0$ (rad)	0.373	0.0081
6	$q_0$ (rad/s)	1.73	0.084
7	$r_0$ (rad/s)	-0.97	0.060
8	$C_x$	-0.100	0.0022
9	$C_{z\dot{\zeta}}$	-3.54	0.24
10	$C_{z\dot{\zeta}^3}$	-	-
11	$C_{m\dot{\zeta}}$	-3.29	0.029
12	$C_{m\dot{\zeta}^3}$	-	-
13	$C_{mq}$	-58.0	4.2

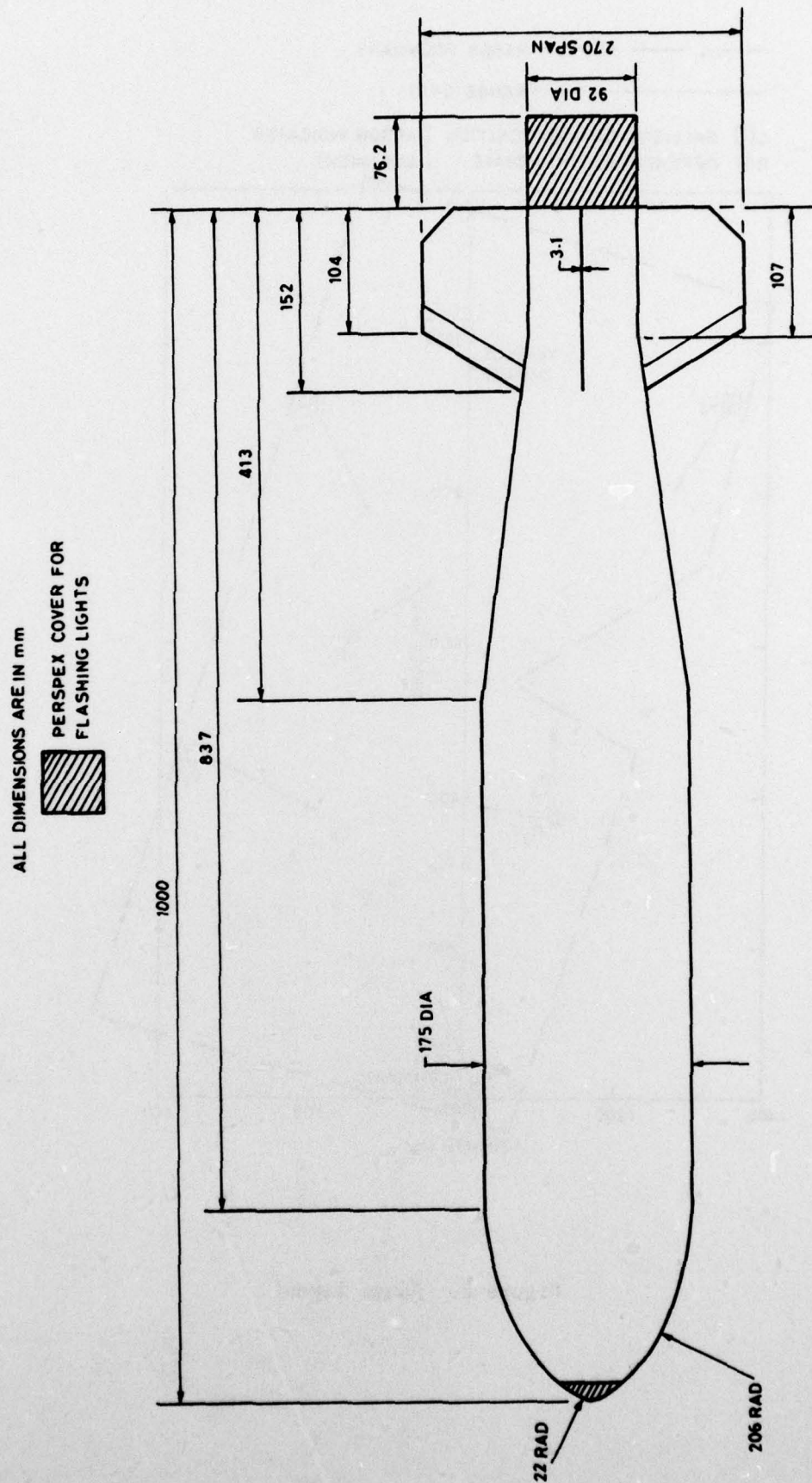


Figure 1. Test vehicle

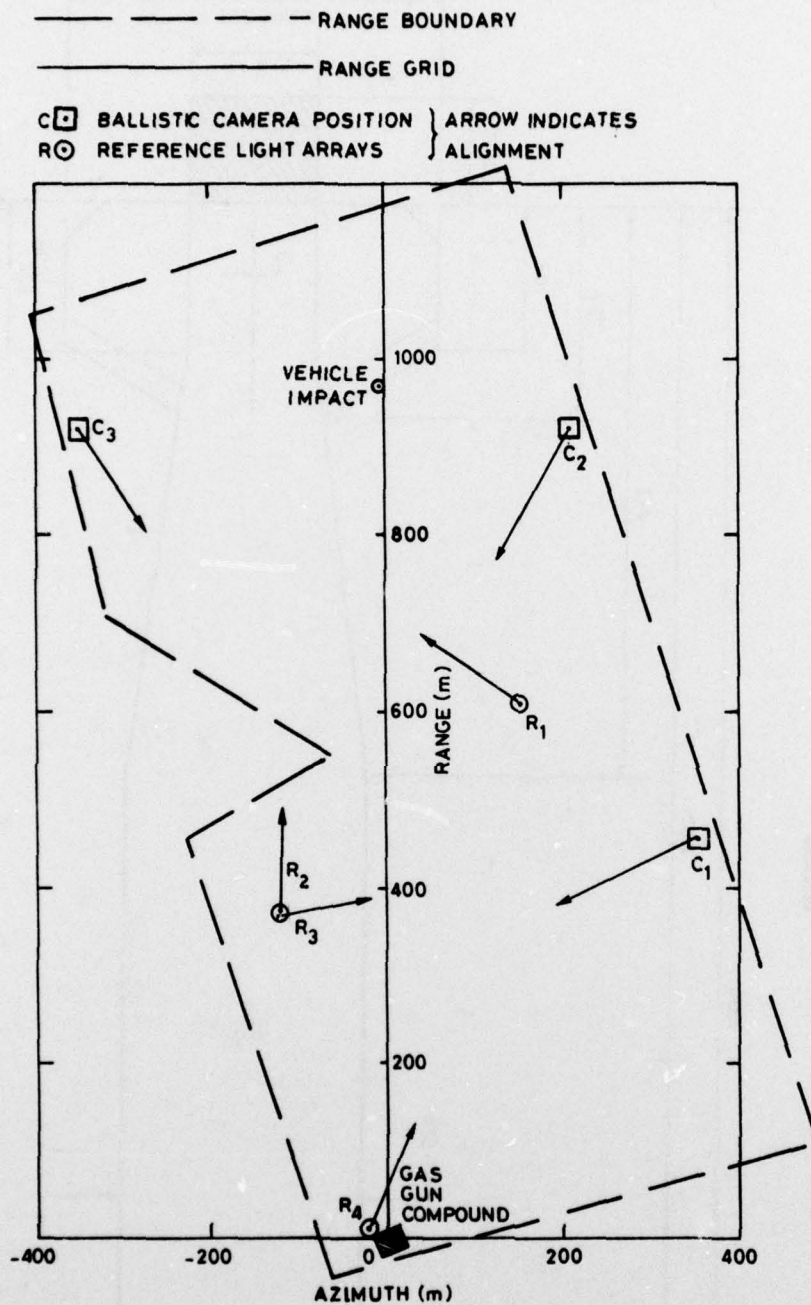


Figure 2. Range layout

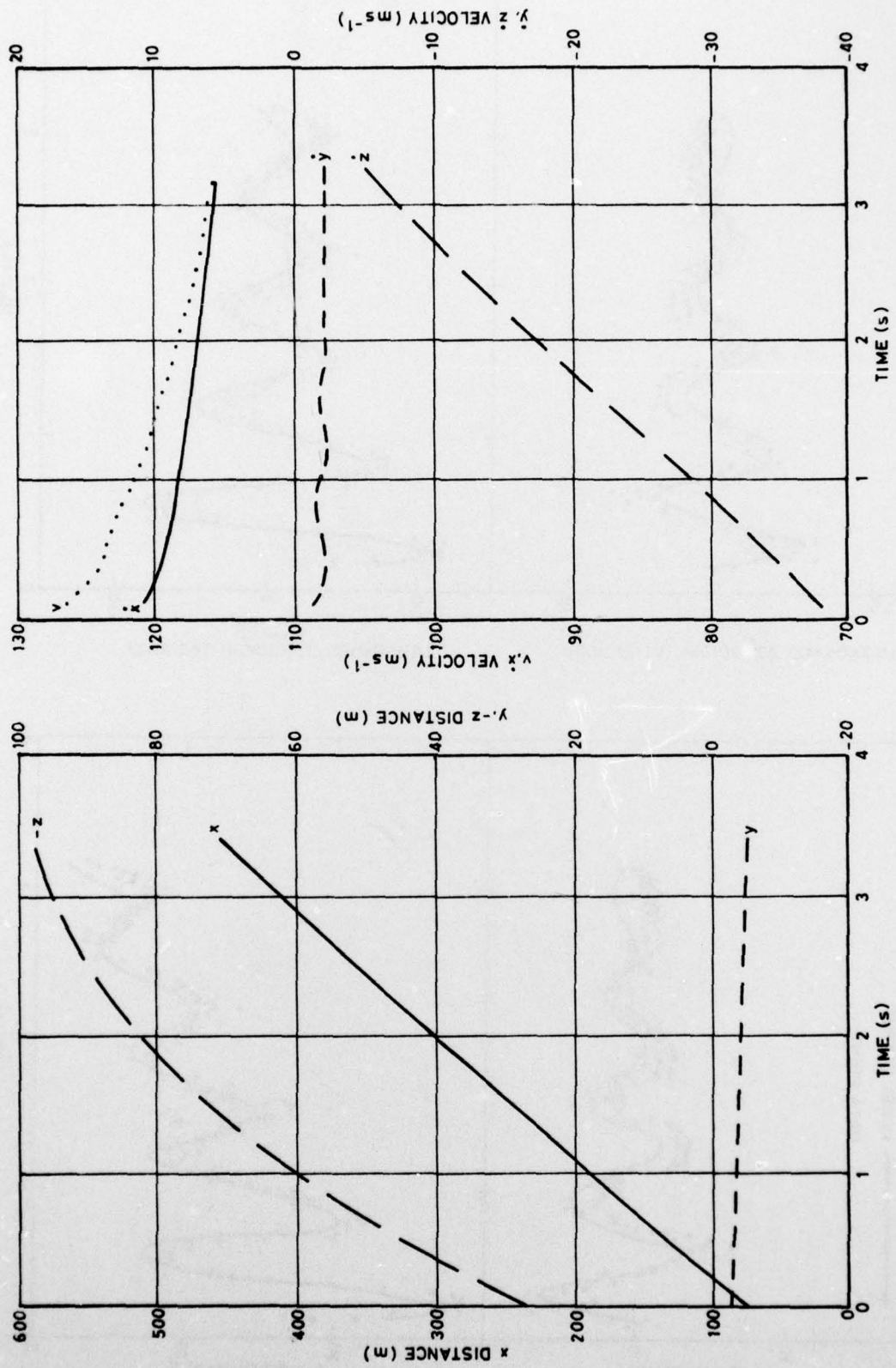


Figure 3. Trajectory of vehicle

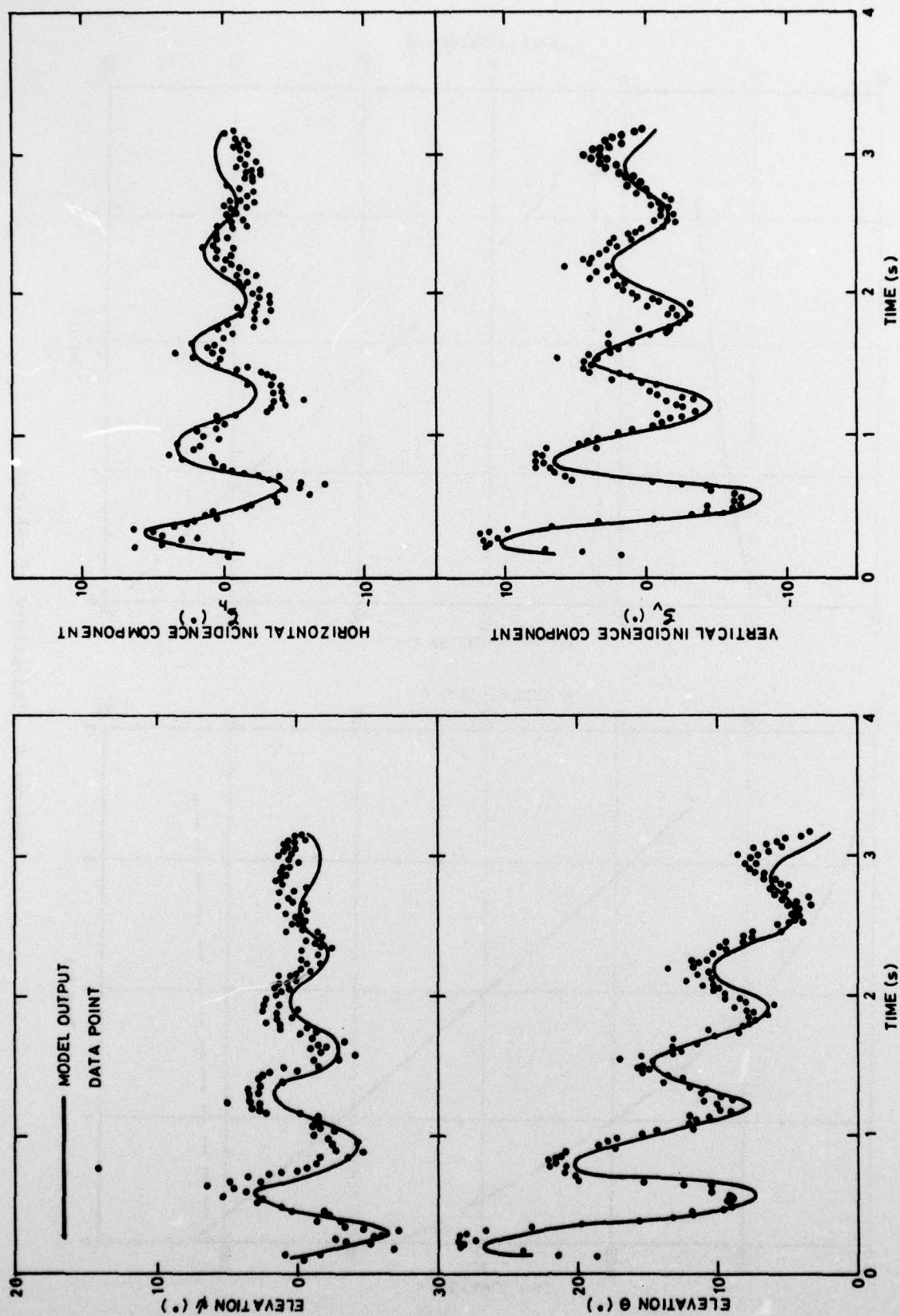


Figure 4. Attitude and incidence histories

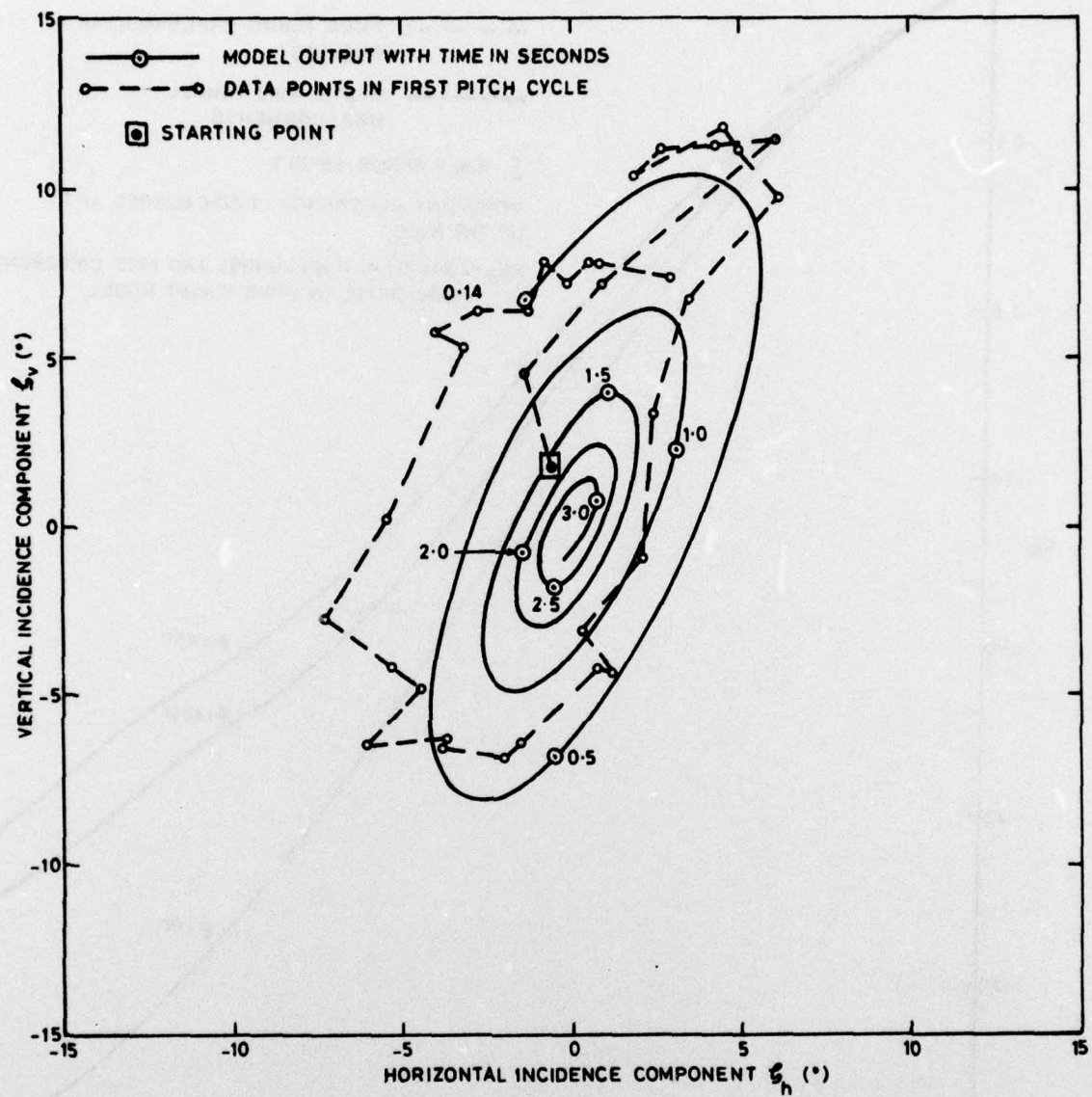


Figure 5. Incidence behaviour

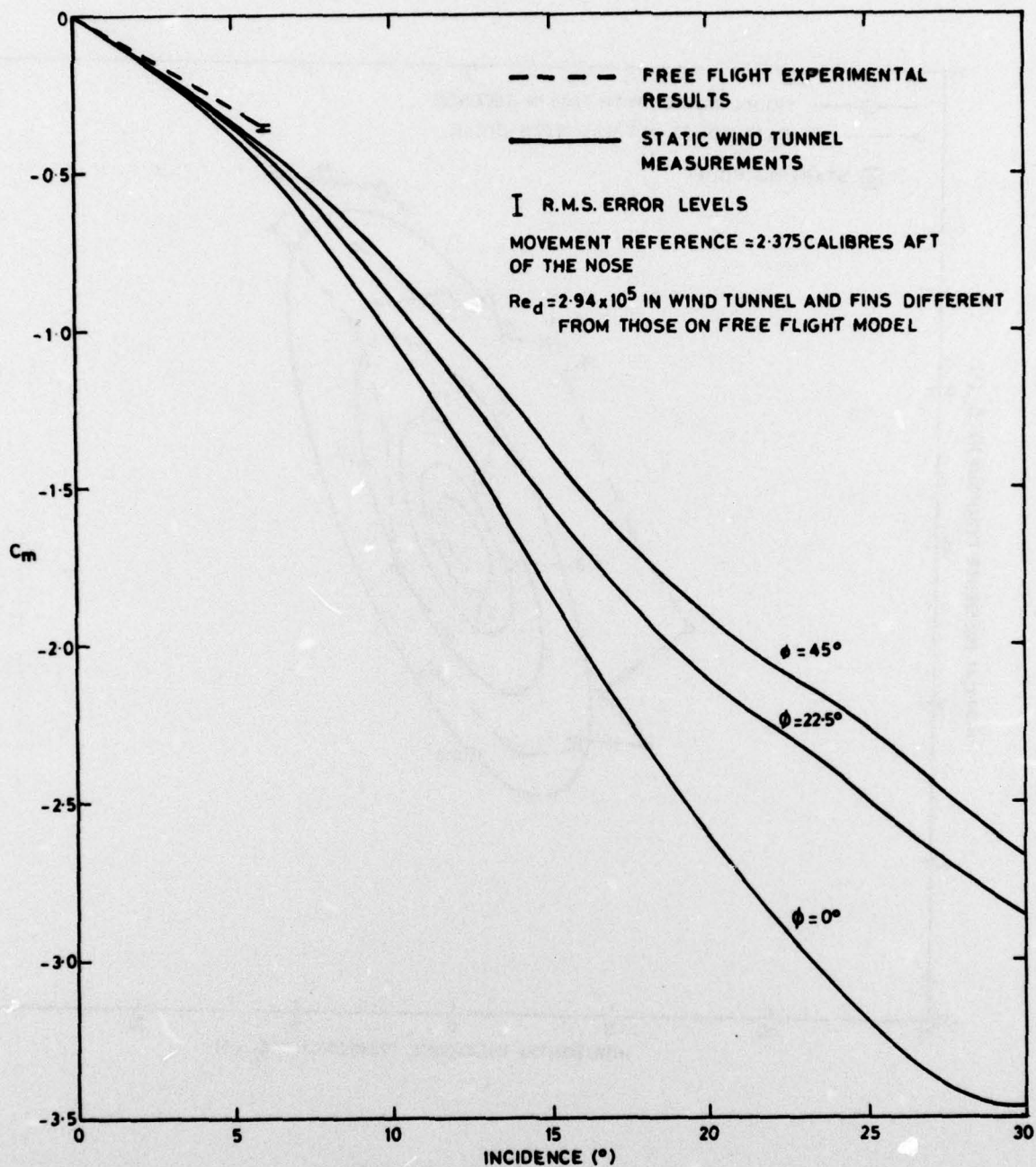


Figure 6. Pitching moment coefficient

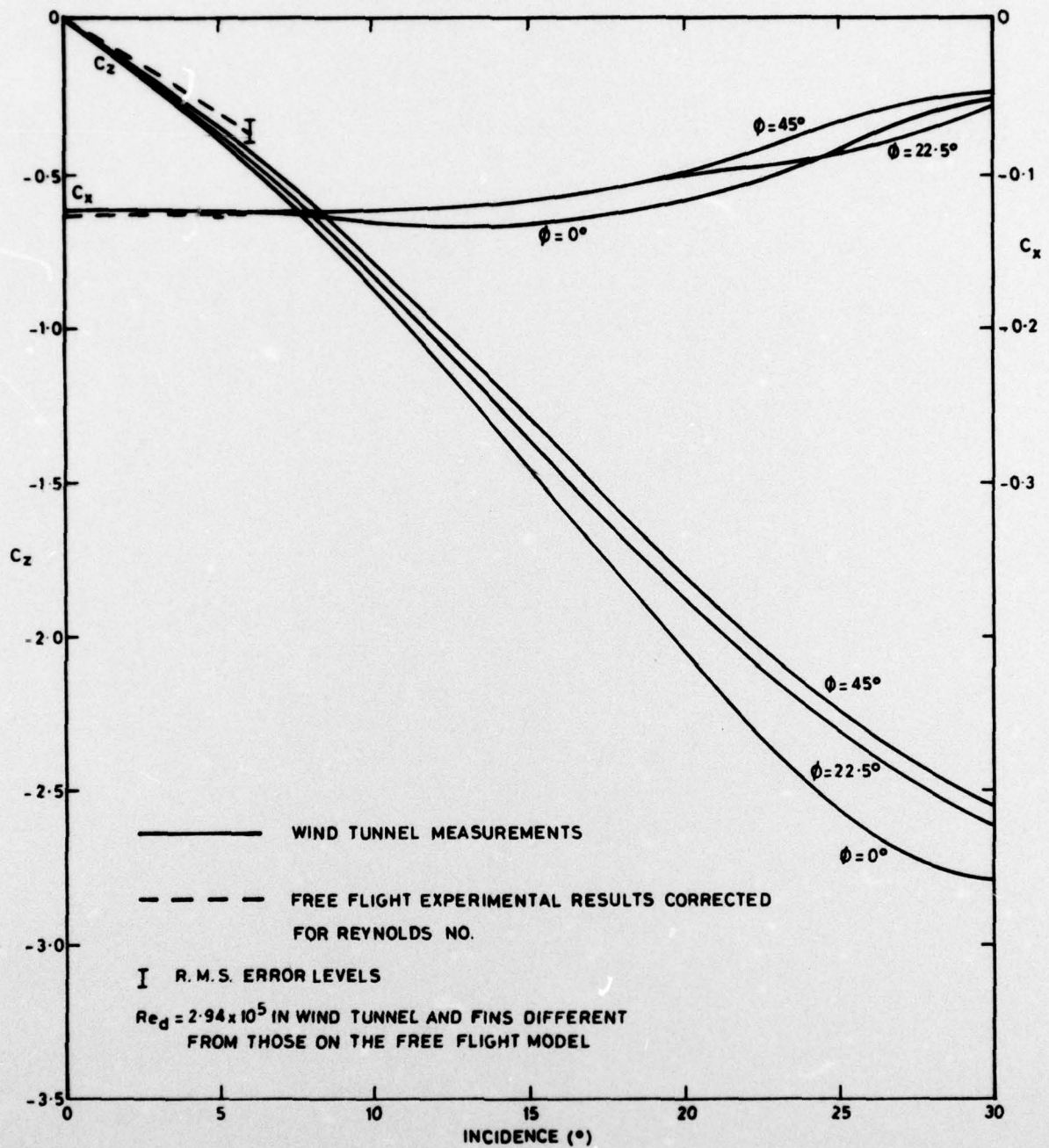


Figure 7. Axial and normal force coefficients

## DISTRIBUTION

## EXTERNAL

## Copy No.

## In United Kingdom

Defence Scientific and Technical Representative, London	1
R.A.E.,	
Aero Department	2 - 3
Space Department	4
Weapons Department	5 - 6
E.G. Cane	7 - 9
Bedford	10
Library	11
R.A.R.D.E.	12
T.T.C.P., U.K. National Leader Panel W-2	13 - 16
Aeronautical Research Council	17 - 18
Aircraft Research Association (Bedford)	19
C.A.A.R.C. Secretary	20
National Lending Library of Science and Technology	21
Royal Aeronautical Society, Library	22

## In United States of America

Counsellor, Defence Science, Washington	23
Defence Research and Development Attache, Washington	24
Air Force Armament Testing Laboratory	25
Ballistics Research Laboratories	26
C.H. Murphy	27
Edgewood Arsenal	28
Eglin Air Force Base	29
N.A.S.A.	30 - 33
Naval Surface Weapons Center	
Dahlgren	34
White Oak	35
Naval Weapons Center	36
Naval Ship Research and Development Center	37
Picatinny Arsenal	38
Redstone Arsenal	39
T.T.C.P. U.S. National Leader Panel W-2	40 - 43
Wright-Patterson Air Force Base, Library	44
American Institute of Aeronautics and Astronautics, Library	45
Pacific Technical Information Services, Northrop Institute of Technology	46

	Copy No.
Applied Mechanics Reviews	47
Arnold Engineering Development Center	48
A.R.O. Incorporated	49
Sandia Corporation, Library	50
<b>In Canada</b>	
Defence Research Establishment, Valcartier	51
N.A.E., Ottawa	52
T.T.C.P., Canadian National Leader Panel W-2	53 - 56
University of Toronto, Institute of Aerospace Studies	57
<b>In Europe</b>	
A.G.A.R.D., Brussels	58 - 63
<b>In India</b>	
Aeronautical Development Establishment, Bangalore	64
Indian Institute of Science, Bangalore (Department of Aero. Engineering)	65
Indian Institute of Technology, Madras (Department of Aero. Engineering)	66
Hindustan Aeronautics Limited, Bangalore	67
National Aeronautical Laboratories, Bangalore	68 - 69
Space Science and Technology Centre, Trivandrum	70
<b>In Australia</b>	
Department of Defence, Canberra	
Defence Library, Campbell Park	71
Air Office	
Air Force Scientific Adviser	72 - 73
Army Office	
Army Scientific Adviser	74 - 75
Navy Office	
Navy Scientific Adviser	76 - 77
Defence Science and Technology	
Chief Defence Scientist	78
Executive Controller, Australian Defence Scientific Service	79
Controller, Policy and Programme Planning Division	80
Superintendent, Defence Science Administration	81
Central Studies Establishment	82

	Copy No.
Assistant Secretary, Scientific and Technical Information	83
For Australian National Library	84
For overseas release to U.K., U.S.A., Canada and New Zealand	85 - 99
Director, Joint Intelligence Organization (DDSTI)	100
B.D.R.S.S., Canberra	101 - 102
Department of Defence, Melbourne	
A.R.L.,	
Chief Superintendent	103
Superintendent, Aerodynamics Division	104
Superintendent, Mechanical Engineering Division	105
Library	106
M.R.L.,	
Library	107
Department of Industry and Commerce, Melbourne	
Government Aircraft Factories	108
R.A.A.F. Academy, Point Cook	109
C.A.C.	110
Institution of Engineers, Australia	111
 INTERNAL	
Director	112
Chief Superintendent, Weapons Research and Development Wing	113
Chief Superintendent, Trials Wing	114
Superintendent, Aerospace Division	115
Head, Ballistics Composite	116
Principal Officer, Dynamics Group	117 - 118
Principal Officer, Aerodynamic Research Group	119 - 120
Principal Officer, Ballistic Studies Group	121
Principal Officer, Field Experiments Group	122 - 123
Principal Officer, Flight Research Group	124 - 125
Principal Officer, Planning and Data Analysis Group	126
Author	127
W.R.E. Library	128 - 129
A.D. Library	130 - 135
Spares	136 - 159

## DOCUMENT-CONTROL DATA

(14) WRE-TN-1719(WR/D)	
1. Security Classification:	2. Establishment, Document, Type, Number, Wing
(a) Complete document: Unclassified	WRE-TN-1719 (WR&D)
(b) Title in isolation: Unclassified	
(c) Summary in isolation: Unclassified	3. Document Date
	(11) Nov 1976 (12) 29 p.

## 4. Title and Sub-title

(6) A NEW TECHNIQUE FOR OBTAINING THE AERODYNAMICS OF MISSILES FROM FLIGHT TRIALS ON A GAS GUN RANGE.

## 5. Personal author(s) (Show affiliations of author(s) if different to issuing establishment)

(10) R.L. Pope (9) Technical note,

6. Corporate Author Weapons Research Establishment

## 7. Summary

✓ This report describes a new method for obtaining the low incidence, linear aerodynamic data for a missile from very simple free flight trials on a gas gun range. The only instrumentation in the free flight model is two flashing lights, one in the nose and one in the tail. The images of these flashing lights are recorded by three ballistic cameras and the positions of the lights can then be calculated very accurately by a least squares solution of the resulting triangulation problem. The velocity of the centre of gravity and the attitude of the vehicle can be estimated from the position measurements for the nose and the tail. A parameter estimation technique using the output error criterion is applied to the attitude and velocity data to obtain aerodynamic terms. The method has been used successfully to estimate axial force, normal force, static stability and pitch damping moment for the test vehicle. ↑

8. Descriptors	9. Cosati Codes
Missiles	2004 1604
Aerodynamics	
Flight tests	10. Task Reference Number
Least squares method	DST 76/011
Computation	
11. Library distribution (Libraries of Australian Defence Group to which copies will be sent)	12. Sponsoring Agency Reference
SW SR AACA	RD73

371700

alt